

Equilibrium properties of an axial next-nearest-neighbor Ising model in two dimensions

A. Sato and F. Matsubara

Department of Applied Physics, Tohoku University, Sendai 980-8579, Japan

(Received 14 May 1999)

We study thermodynamic properties of an axial next-nearest-neighbor Ising model in two dimensions using a cluster heat bath Monte Carlo method. The method drastically reduces the relaxation time, and enables us to study equilibrium properties of the model. We show that the model really exhibits two phase transitions at T_{c1} and $T_{c2} (< T_{c1})$, as predicted by a free fermion approximation. The one at T_{c1} is shown to be of the Kosterlitz-Thouless type, and the other to be of the Pokrovsky-Talapov type. The higher transition temperature T_{c1} is considerably lower than those estimated by previous authors. Low-temperature properties as well as the lower transition temperature T_{c2} are found to be well described by the fermion approximation.

[S0163-1829(99)04438-0]

I. INTRODUCTION

Systems with competitive interactions have been extensively studied in the last two decades, because they have very rich physical properties, including features such as commensurate-incommensurate phase transitions, Lifshitz points, and multiphase points.¹ The axial next-nearest-neighbor Ising (ANNNI) model is one of the simplest realizations of such systems. The two-dimensional ANNNI model consists of ferromagnetic Ising chains coupled by the ferromagnetic nearest-neighbor and antiferromagnetic next-nearest-neighbor interchain interactions. The Hamiltonian is described by

$$H = -J_0 \sum_{x,y} S_{x,y} S_{x+1,y} - J_1 \sum_{x,y} S_{x,y} S_{x,y+1} - J_2 \sum_{x,y} S_{x,y} S_{x,y+2}, \quad (1)$$

where $S_{x,y} = \pm 1$, $J_0 (> 0)$ is the ferromagnetic nearest-neighbor interaction in the chains, and $J_1 (> 0)$ and $J_2 (< 0)$ are the interchain nearest-neighbor and next-nearest-neighbor interactions, respectively. It is well known that the ground state of the model is the ferromagnetic phase for $\kappa (\equiv -J_2/J_1) < \frac{1}{2}$ and the $\langle 2 \rangle$ phase for $\kappa > \frac{1}{2}$ which is described by an alternate arrangement of two up-spin chains and two down-spin chains in the axial direction, i.e., $\cdots + + - - \cdots$.

The properties at finite temperatures have been studied by numerous methods. It is now widely believed that a floating incommensurate (IC) phase characterized by a power law decay of the pair spin correlation appears between the $\langle 2 \rangle$ phase and the paramagnetic phase.^{2,3} However, the transition temperatures have not yet been determined reliably. As for the phase transition between the paramagnetic and IC phases, the transition temperature T_{c1} has been estimated by various methods such as approximation theories,^{4,5} Monte Carlo (MC) simulations,^{2,6,7} a high-temperature-series expansion,⁸ a finite-size scaling of correlation length,⁹ a phenomenological renormalization,¹⁰ and a dynamical MC method.¹¹ However, their results scatter as $T_{c1}/J_1 = 1.2 \sim 1.8$ for $\kappa = 0.6$. Moreover, no evidence has yet been given for whether the transition really belongs to the universality class of the

Kosterlitz-Thouless (KT) transition.¹² For the phase transition between IC and $\langle 2 \rangle$ phases, two analytic methods were applied for estimating its transition temperature T_{c2} . One is a fermion approximation which assumes that the IC phase near above the $\langle 2 \rangle$ phase consists of regions of different $\langle 2 \rangle$ spin configurations separated by $+++$ or $---$ domain walls which run along the chain direction.^{3,13} The other is the interface free energy method of Müller-Hartmann and Zittartz (MHZ),¹⁴ which assumes that the interface runs along the direction (axial direction) perpendicular to the chains.¹⁵ The latter method gives a higher transition temperature than the former. Numerical calculations reported so far^{6,9,10} supported the MHZ result. This fact is rather strange, because the interface that brings the phase transition from the $\langle 2 \rangle$ phase to the IC phase is likely to run along the chain direction, as assumed in the fermion approximation.

The difficulty of examining the ANNNI model lies in the lack of an appropriate method. In the MC method, due to a very long relaxation time, no equilibrium quantity has yet been obtained for large lattices. One often measured the melting temperature of the $\langle 2 \rangle$ phase and the peak temperature of the specific heat to estimate T_{c2} and T_{c1} , respectively.⁶ However, the former gives nothing but an upper bound of T_{c2} , and the latter is a characteristic temperature around which the short-range order develops. In the transfer-matrix method, the lattices of $M \times \infty$ are treated where $M \leq 8$ or $M \leq 16$ when the method is applied in the axial¹⁰ or chain⁹ direction, respectively. Of course, those numbers of M would not be large enough for analyzing models with complex structures.

In this paper, we develop a powerful method for treating the model on larger lattices, and study its equilibrium properties for $\kappa > 1/2$. Attention is paid to the nature of both phase transitions as well as their temperatures T_{c1} and T_{c2} . Using the method, we obtain equilibrium values of physical quantities of interest for different sizes of the lattice. Then we determine the values of T_{c1} and T_{c2} to a good accuracy with the aid of finite-size scaling analyses. We find that the phase transition at T_{c1} is well described by the KT theory,¹² and that at T_{c2} by the fermion approximation.^{3,13} The method is described in Sec. II. Results are presented in Sec. III and analyzed in Sec. IV. Section V is devoted to conclusions. A brief report of the method was already given in Ref. 18.

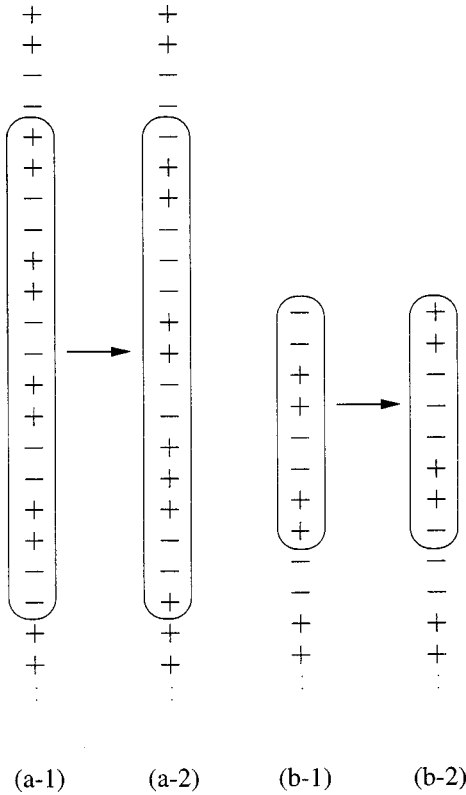


FIG. 1. Spin configurations of the ANNNI model. The symbols + and - mean the chains with up and down spins, respectively.

II. METHOD

We examine the ANNNI model in two dimensions using the MC method.

A. Difficulty in the MC simulation

The difficulty in the conventional MC method lies in the fact that the spin configuration obtained in this method at low temperatures depends on initial spin configurations. This is because the spin configuration of the IC phase at temperatures near T_{c2} consists of regions of the $\langle 2 \rangle$ phase separated by +++ or --- domain walls.^{3,7} We consider the process of the $\langle 2 \rangle$ phase melting to the IC phase. The spin configuration of the $\langle 2 \rangle$ phase is schematically depicted in (a-1) of Fig. 1. In this case, every chain is stable, because it has an interchain coupling energy of $2J_2L_x (< 0)$, where L_x is the number of the spins on each chain. Suppose all the spins on one chain in (a-1) are flipped yielding one domain wall. This change brings two unstable chains with positive interchain coupling energies of $-2J_2L_x$ and $2(J_1 + J_2)L_x$. Then, even if this spin configuration is realized by chance, it will come back quickly to the old spin configuration (a-1). A spin configuration that contains no chain with a positive interchain coupling energy is a sequence of blocks of two or three chains with the same spin direction such as $\dots ++ --- ++ --- ++ \dots$. To obtain the IC phase starting from the $\langle 2 \rangle$ phase, we must insert four domain walls simultaneously as illustrated in (a-2) of Fig. 1. Therefore, we must rearrange at least $16L_x$ spins, which is not easy to be realized by using the conventional single-spin-flip MC method.

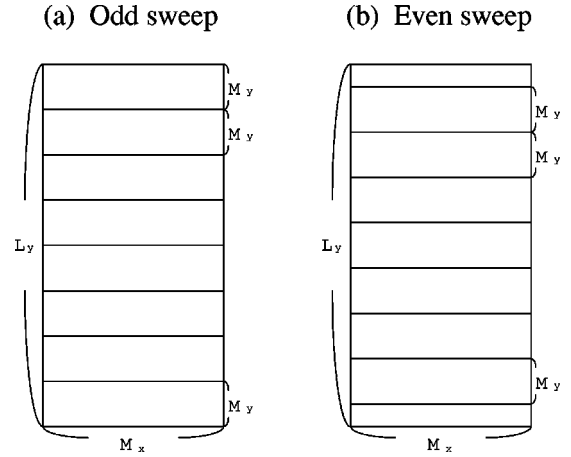


FIG. 2. Two ways of division of the lattice into clusters.

This difficulty is not largely relieved even when one chooses an open boundary condition, because open boundaries lead to a pinning effect,¹⁶ i.e., the end two chains tend to take either ++ or -- spin configuration. In this case, we must rearrange at least $8L_x$ spins at the ends as shown in (b-1) and (b-2) of Fig. 1. Thus the ANNNI model is one of the most difficult models in the computer simulation.

B. CHB method

Recently, we found an algorithm called the cluster heat bath (CHB) method,^{17,18} which enables us to update the spin configuration of a block (cluster) of the spins with the aid of the transfer matrix method. The CHB method is particularly effective for simulating the ANNNI model, because we can choose clusters of $M_y \times L_x$ spins.¹⁸

We describe the procedure of applying the CHB method to the ANNNI model in two dimensions. For simplicity, we consider the lattice consisting of $L_y = 2L$ chains with $L_x = L$ spins, i.e., the lattice with $L_x \times L_y = L \times 2L$ spins, and L is chosen to be a multiple of 4. A periodic boundary condition is imposed on the chains (the x direction) and an open boundary condition in the axial direction (the y direction). The latter boundary condition is used so as to reduce the relaxation time. We choose the cluster of $M_y = 8$ chains. We decompose the lattice into either of the two sets of the clusters shown in Fig. 2. The decompositions (a) and (b) are used for odd and even MC sweeps, respectively. The spin configuration for every cluster is updated in order by applying the CHB algorithm. In this procedure, we may add the domain walls at both ends in the odd sweep and put them inside the lattice, and vice versa.

In the application of the CHB algorithm, we further decompose each cluster into a set of L layers of M_y spins, so that the spins on each layer interact only with the spins on the adjacent layers. In updating the spin configuration in a cluster, we must give a spin configuration of one layer, because the algorithm works for systems having boundaries. This layer is chosen at random and its spin configuration is left unchanged. The spin configurations of the remaining $(L - 1)$ layers are updated step by step by using their Boltzmann weights.¹⁸

To examine the validity of the method, we first make simulations using both the conventional MC method and the

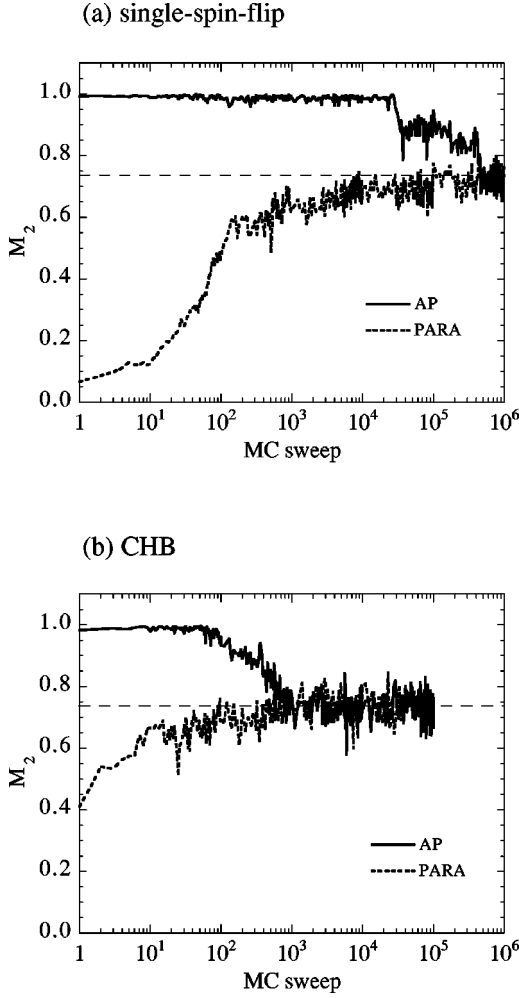


FIG. 3. The MC sweep dependences of the square of the chain magnetization M_2 at $T=1.0J_1$ starting with two initial spin configurations of a paramagnetic phase (PARA) and the $\langle 2 \rangle$ phase (AP) by (a) the conventional MC method and (b) the CHB method. The broken line indicates the equilibrium value.

CHB method starting with two different initial conditions, i.e., a paramagnetic spin configuration and the $\langle 2 \rangle$ spin configuration. In Fig. 3, we present typical examples of the MC sweep dependence of the square M_2 of the chain magnetization,

$$M_2 = \frac{1}{2L} \sum_{y=1}^{2L} \left(\frac{1}{L} \sum_{x=1}^L S_{x,y} \right)^2. \quad (2)$$

In the CHB method, about 1000 MC sweeps are necessary for the two runs to obtain the same value. In contrast to this, in the conventional MC method, MC sweeps about 1000 times larger are necessary. This difference in the number of the MC sweeps becomes larger as the temperature is decreased and/or the size of the lattice is increased. Note, in the CHB method, about 30 times as much CPU time is necessary for every MC sweep.

III. RESULTS

In this paper, we examine the ANNNI model with $J_0 = J_1$ and $\kappa > 1/2$ for which the $\langle 2 \rangle$ phase is realized at low

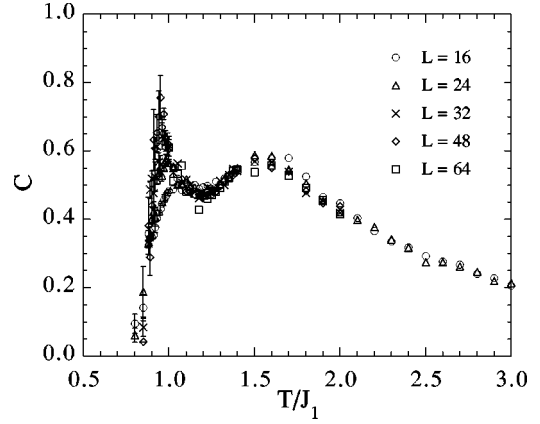


FIG. 4. The temperature dependence of the specific heat C for different sizes of the lattice. Error bars are attached only for data for $T \leq 1.0J_1$.

temperatures. We calculate the specific heat C , the average value of the square of the chain magnetization $\langle M_2 \rangle$, and the spin correlation in the axial direction $\langle S_0 S_y \rangle$. These are defined as

$$C = \frac{1}{2T^2 L^2} (\langle E^2 \rangle - \langle E \rangle^2), \quad (3)$$

$$\langle M_2 \rangle = \frac{1}{2L} \sum_{y=1}^{2L} \left\langle \left(\frac{1}{L} \sum_{x=1}^L S_{x,y} \right)^2 \right\rangle, \quad (4)$$

$$\langle S_0 S_y \rangle = \frac{1}{L} \sum_{x=1}^L \frac{1}{2L-y} \sum_{y'=1}^{2L-y} \langle S_{x,y'} S_{x,y'+y} \rangle, \quad (5)$$

where E is the energy and $\langle \dots \rangle$ is the MC sweep average. Hereafter, we measure the temperature in units of the Boltzmann constant $k_B = 1$. The size of the lattice is from 8×16 to 64×128 , i.e., $L = 8 \sim 64$. The MC sweeps are about 200 000 for the largest lattice. Data for about five independent runs are averaged for each size of the lattice. Here detailed results are presented in the case of $\kappa = 0.6 (J_2 = -0.6J_1)$.

The temperature dependence of the specific heat is presented in Fig. 4. It exhibits a double peak. The one which occurs at a higher temperature of $T \sim 1.5J_1$ is very broad and almost independent of the lattice size L . The other, occurring at $T \sim 0.9J_1$, is rather sharp and exhibits a size dependence implying the occurrence of a phase transition.

The temperature dependence of $\langle M_2 \rangle$ is presented in Fig. 5. As the temperature is decreased, it exhibits a rapid increase below $T \sim 1.5J_1$ and saturates around $T \sim 0.9J_1$. A remarkable size dependence is seen for $T > 0.9J_1$ revealing the decay of the spin correlation even in the chain direction.

The spin correlation $\langle S_0 S_y \rangle$ in the axial direction is presented in Fig. 6. It exhibits an oscillatory decay. The decay rate becomes smaller as the temperature is decreased and the period of the oscillation decreases towards 4, revealing the occurrence of the $\langle 2 \rangle$ phase. A weak beat is seen at low temperatures. The phase of the oscillation changes at necks. This fact confirms the suggestion that the spin structure of the IC phase just above the $\langle 2 \rangle$ phase may be described by a periodic arrangement of domain walls.

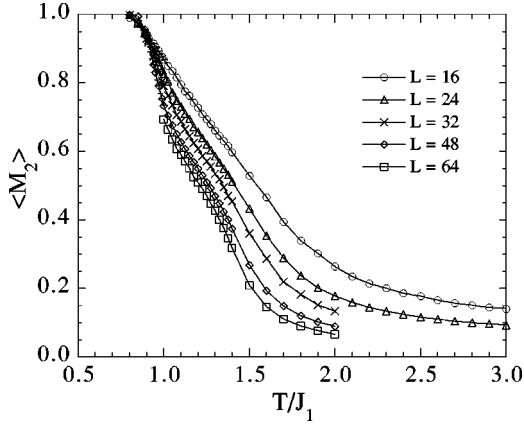


FIG. 5. The temperature dependence of the square of the chain magnetization $\langle M_2 \rangle$ for different sizes of the lattice. Error bars are smaller than symbols.

IV. PHASE TRANSITION

Now we discuss the phase transitions at the higher and lower temperatures T_{c1} and T_{c2} . It has been believed that the phase transition between the paramagnetic and the IC phases is of the KT¹² type, and the other transition is of the Pokrovsky-Talapov type.¹⁹ However, the transition tempera-

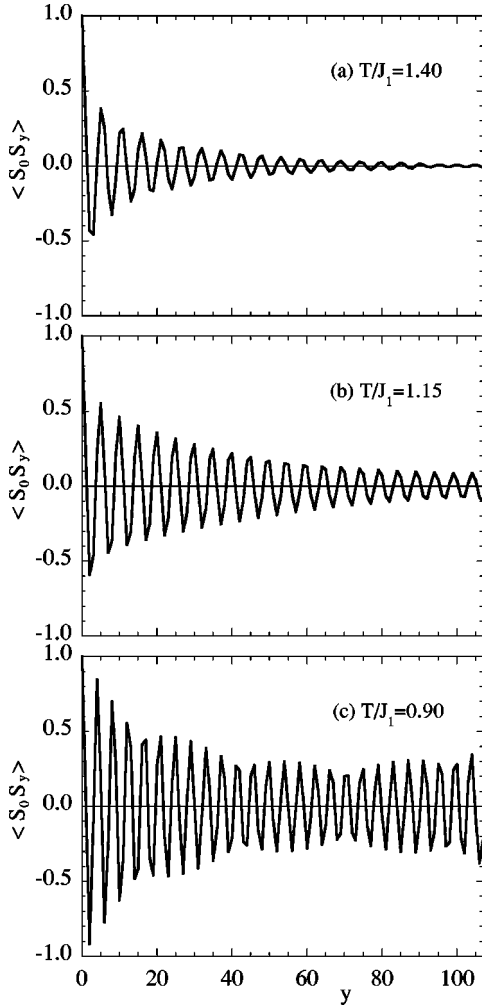


FIG. 6. The spin correlation function $\langle S_0 S_y \rangle$ for the lattice 64×128 .

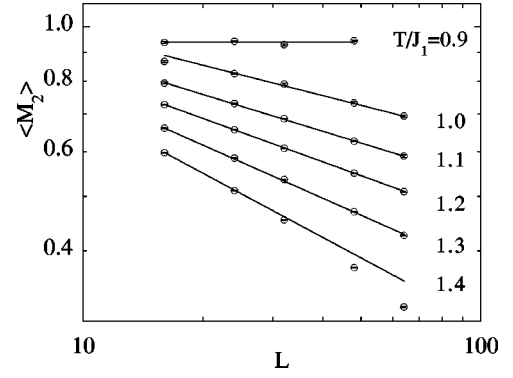


FIG. 7. $\langle M_2 \rangle$ for fixed temperatures as functions of L .

tures have not yet been settled. We examine properties of those phase transitions and the transition temperatures analyzing the results presented in Sec. III.

A. KT-like phase transition

First we consider phase transition at the higher temperature T_{c1} . If the IC phase has a nature of the KT phase, the spin correlation function decays according to the power law

$$\langle S_{0,0} S_{x,y} \rangle \sim r^{-\eta} \cos(qy) \quad \text{for } x, y \gg 1, \quad (6)$$

with $r = \sqrt{x^2 + y^2}$. Here η and q are the decay exponent and the wave number, respectively. Then the square of the chain magnetization becomes

$$\langle M_2 \rangle = \frac{1}{2L^2} \sum_{y=1}^{2L} \sum_{x=1}^L \langle S_{1,y} S_{x,y} \rangle \sim L^{-\eta}. \quad (7)$$

Thus, if we plot $\langle M_2 \rangle$ as a function of L on a log-log scale, the data at the same temperature will lie on a straight line. We show the results in Fig. 7. In fact, the data for $T \leq 1.20J_1$ seem to lie on a straight line. We have estimated values of the decay exponent η for different temperatures using the least-square method. The results are plotted in Fig. 8 as a function of the temperature. As the temperature is decreased, η decreases monotonously and its error bar becomes smaller. The declination becomes smaller and seems to be almost constant around $T = 1.20J_1$. As the temperature is decreased further, a change in the declination is seen

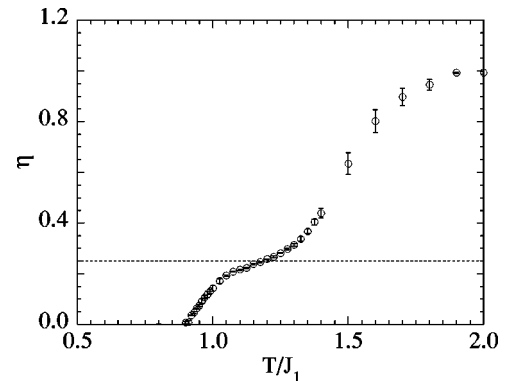
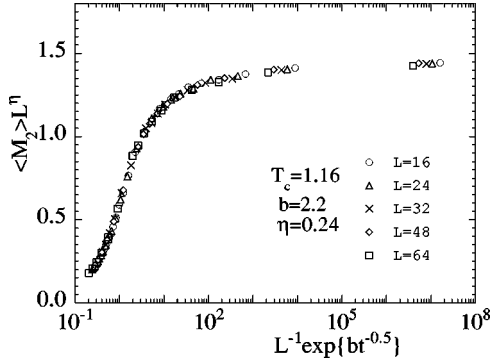


FIG. 8. The temperature dependence of the decay exponent η in the chain direction. The dotted line indicates the KT criterion of $\eta = 1/4$.

FIG. 9. A typical result of the scaling plot of $\langle M_2 \rangle$.

around $T = 1.00J_1$. Finally, $\eta = 0$ around $T = 0.90J_1$ suggesting the occurrence of the $\langle 2 \rangle$ phase. It is very interesting to notice that, at the characteristic temperature $T = 1.20J_1$, $\eta \sim 1/4$ which is the criterion of the KT phase transition. The error bars are very small below this temperature, suggesting the occurrence of the KT phase. To confirm this finding, we make a scaling analysis. If the correlation length diverges as¹²

$$\xi \sim \exp(bt^{-0.5}), \quad (8)$$

with $t = (T - T_{c1})/T_{c1}$ and b being some constant, $\langle M_2 \rangle$ may be scaled as

$$\langle M_2 \rangle L^\eta = Y[L^{-1} \exp(bt^{-0.5})], \quad (9)$$

where Y is some scaling function. A typical result is shown in Fig. 9. We can obtain a good scaling plot when we choose

$$T_{c1}/J_1 = 1.16 \pm 0.04, \quad (10)$$

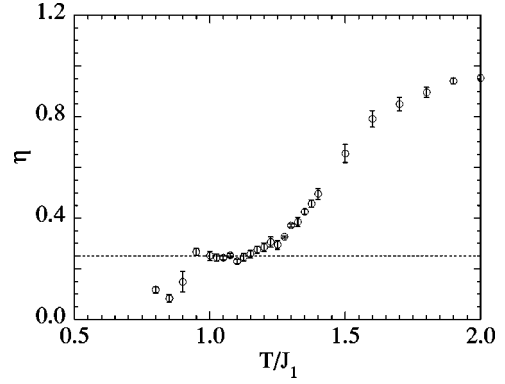
$$\eta = 0.25 \pm 0.02. \quad (11)$$

The most interesting point is that the estimated value of $\eta \sim 0.25$ is just the same as that of the KT criterion.¹²

Next we examine the spin correlation in the axial direction. The analysis is more difficult than that in the chain direction, and results are less accurate, because the spin correlation decays oscillatory and much CPU time is necessary to obtain the data with good accuracy. In addition, to obtain reliable results we must treat larger lattices because the relation of Eq. (6) holds for $y \gg 1$. A conventional way to estimate the decay constant is to fit the data to Eq. (6) using the least-square method. Another way is to make the Fourier translation of the data. We have made both analyses, but these were not so effective, because we could use the data of $\langle S_0 S_y \rangle$ only in a limited range of y ($2L \gg y \gg 1$). Here, to estimate η , we consider an integrated quantity $\langle K_L \rangle$ which is similar to $\langle M_2 \rangle$:

$$\langle K_L \rangle = \frac{4}{L^3} \sum_{x=1}^L \sum_{y_1=L/2+1}^L \sum_{y_2=y_1+1}^{y_1+L/2} |\langle S_{x,y_1} S_{x,y_2} \rangle|. \quad (12)$$

Here we only use the data in the inner part $L \times L$ of the $L \times 2L$ lattice, because we treat the lattice with open boundaries. We make the same estimation of η as in the case of the chain direction, and plot the results as a function of the temperature in Fig. 10. We find a temperature dependence similar to that in the chain direction. Especially, as the tempera-

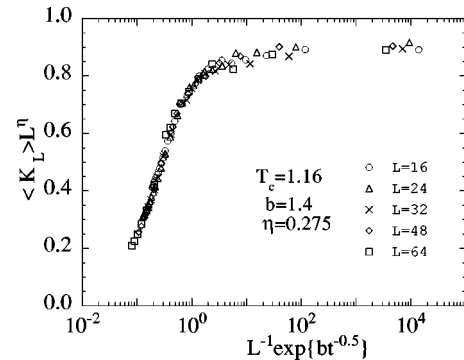
FIG. 10. The temperature dependence of the decay exponent η in the axial direction. The dotted line indicates the KT criterion of $\eta = 1/4$.

ture is decreased, η becomes $1/4$ around $T = T_{c1} \sim 1.16J_1$. However, it stays $\eta \sim 1/4$ down to $T \sim 0.95J_1$ in contrast with the monotonous decrease in the chain direction. This difference in the value of η between the two directions is likely to come from the spin structure near the transition to the $\langle 2 \rangle$ phase, i.e., it consists of regions of the $\langle 2 \rangle$ phase separated by the $+++$ or $---$ domain walls. We also make the scaling analysis of $\langle K_L \rangle$ assuming the same scaling relation as $\langle M_2 \rangle$ but with different values of η , T_{c1} , and b . Unfortunately, because of the scattering of the data, it was not easy to estimate those values definitely without any preconception. But, putting the same value of $T_{c1} = 1.16J_1$, we can fit the data fairly well as shown in Fig. 11. The value of $\eta \sim 0.27$ is also compatible with that in the chain direction. Thus we may conclude that the phase transition between the paramagnetic phase and the IC phase belongs to the same universality class of the KT phase transition. We should note that the value $T_{c1} \sim 1.16J_1$ is lower than any of previous estimations.^{4-6,8-10}

B. Lower-temperature phase transition

Next we consider the phase transition at T_{c2} . In this temperature range, it is natural to consider the density $\langle n_L \rangle$ of the domain walls. We can readily calculate it for the finite lattice as follows:

$$\langle n_L \rangle = \frac{1}{L} \sum_{x=1}^L \frac{2 \times [(L-1) - \langle m(x) \rangle]}{2L}, \quad (13)$$

FIG. 11. A typical result of the scaling plot of $\langle K_L \rangle$.

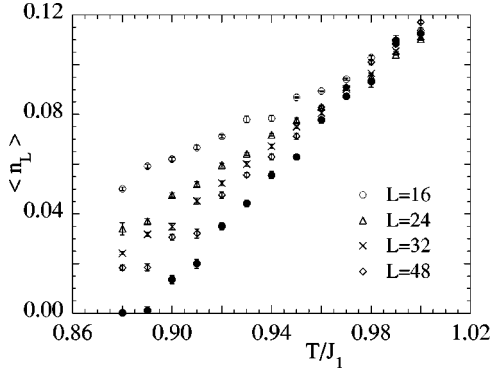


FIG. 12. The temperature dependences of the density $\langle n_L \rangle$ of the domain walls for different sizes of the lattice. Closed circles indicate extrapolated values.

where $m(x)$ is the number of spin pairs for x th column which has different signs. The temperature dependencies of $\langle n_L \rangle$ for different L are shown in Fig. 12. As the temperature is decreased, the size dependence becomes remarkable below $T \sim 1.0J_1$. After several trials, we have found that the data fit well by $\langle n_L \rangle - 1/L$. The results of the extrapolation to $L \rightarrow \infty$ are also plotted in the figure.

The extrapolated value becomes $\langle n \rangle = 0$ around $T = 0.89J_1$, which suggests $T_{c2} \sim 0.89J_1$. This result is consistent with that estimated from the behavior of the chain magnetization. But the data for $T \sim 0.90J_1$ round. Then we examine the temperature dependence of $\langle n_L \rangle$ at $T \sim T_{c2}$ using a scaling analysis. Since the fermion approximation suggested that $\langle n \rangle$ vanishes in proportion to $(T - T_{c2})^\beta$ with $\beta = 1/2$,³ we suppose that $\langle n \rangle$ and the correlation length ξ may be expressed as

$$\langle n \rangle \sim (T - T_{c2})^\beta, \quad (14)$$

$$\xi \sim (T - T_{c2})^{-\nu}. \quad (15)$$

Then the data for different L will be scaled as

$$\langle n_L \rangle L^{\beta/\nu} = F(L^{1/\nu} t), \quad (16)$$

with $t = (T - T_{c2})/T_{c2}$. Putting $\beta = 1/2$, we try to fit the data and find that a good scaling plot is obtained when $T_{c2}/J_1 \sim 0.91$ and $\nu \sim 1.0$. A typical result is shown in Fig. 13. We suggest, hence, that a usual second-order phase transition occurs at the lower transition temperature of $T_{c2} \sim 0.91J_1$. This transition temperature is very close to the results of the

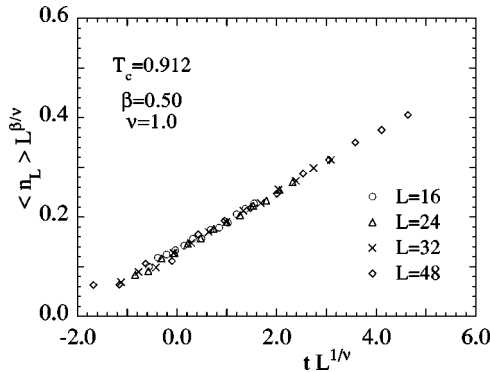


FIG. 13. A typical result of the scaling plot of $\langle n_L \rangle$.

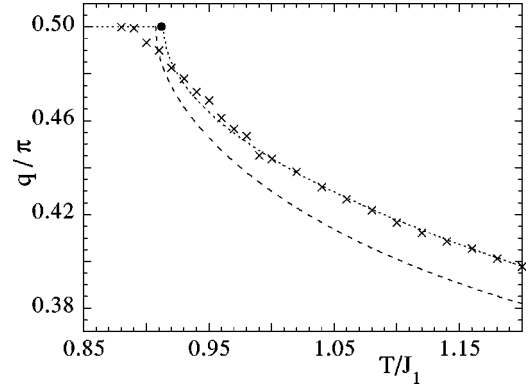


FIG. 14. The temperature dependence of the wave vector q together with those of the fermion approximations. The broken and dotted curves are those of the VB and GC approximations, respectively, and the closed circle indicates the result of the finite-size scaling analysis.

fermion approximations, i.e., $T_{c2} \sim 0.907J_1$ by Villain and Bak (VB)³ and $T_{c2} \sim 0.914J_1$ by Grynberg and Ceva (GC),¹³ but considerably different from that of the MHZ method of $T_{c2} \sim 1.10J_1$.¹⁵ We note that the previous application of the MHZ method is not appropriate, because it considers the interface along the axial direction. If we consider the creation of domain walls along the chain direction as considered in the fermion approximations, we obtain a similar value of $T_{c2} \sim 0.906J_1$ (see the Appendix). We also note that a cluster variation method by Murai *et al.*⁵ gives a close value of $T_{c2} \sim 0.91J_1$, although the method gives a different values of $T_{c1} \sim 1.56J_1$ for the other phase transition.

Finally, we compare our result with those of the fermion approximation. We estimate the wave vector q from

$$q = \frac{1 - \langle n \rangle}{2} \pi, \quad (17)$$

and plot it in Fig. 14 as a function of the temperature together with those of the fermion approximations. Agreements between our MC result and those approximation results are very good. Especially, our result reproduces GC's result excellently up to $T \sim T_{c1}$. We conclude, hence, that the present MC study supports the picture of the IC phase in the fermion approximations. We should make a comment. The fermion approximation of GC seems to give a better result than the free fermion approximation of VB, because it takes into account an interaction between the fermions. In fact, in the case of $\kappa = 0.6$, a better agreement with the MC result is obtained in the GC's approximation. However, as κ increases, the deviation of GC's result from the MC result increases faster than that of VB's result. For larger κ , as will be shown in Sec. IV C, the agreement with the MC result is rather better in the VB's approximation and still better in our MHZ theory.

C. Phase diagram

We have also examined the model with different values of κ . The decay exponent η and the domain wall density $\langle n \rangle$ estimated by using the least-square method are plotted in Figs. 15 and 16, respectively, as functions of the tempera-

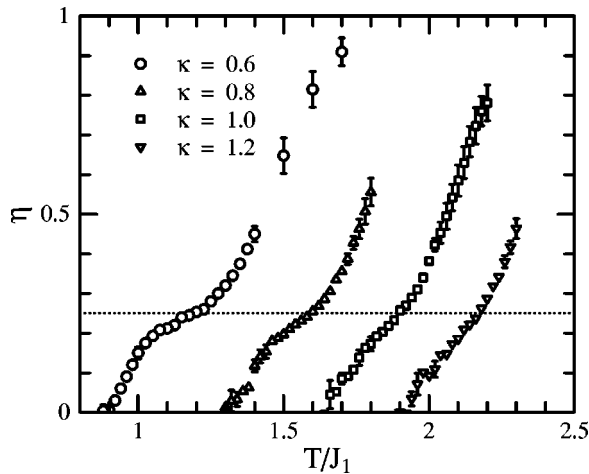


FIG. 15. The temperature dependences of the decay exponent η in the chain direction for different κ . The dotted line indicates the KT criterion of $\eta=1/4$.

ture. From the results, we give the phase diagram shown in Fig. 17. Here we plot T_{c1} 's estimated from the KT criterion of $\eta=1/4$ and T_{c2} 's from the condition of $\langle n \rangle = 0$. It is noted, however, that we have confirmed those values using the same scaling analyses as made in Secs. IV A and B. The most important point is that, in contrast with the previous results, the IC phase appears in a small temperature range above the $\langle 2 \rangle$ phase. It should be noted again that the fermion approximations (and our MHZ theory) give values of T_{c2} very close to that of the MC result. On the other hand, the transition temperature T_{c2} estimated by the previous MHZ theory is rather close to the higher transition temperature T_{c1} . These results are not unexpected. Suppose that several domain walls along the chain direction are created in the $\langle 2 \rangle$ phase. Then the $\langle 2 \rangle$ phase is destroyed, but a strong spin correlation along the chain still remains. Since, as seen above, the IC phase just above the $\langle 2 \rangle$ phase has this spin structure, the fermion approximations (and our MHZ theory) give the lower transition temperature T_{c2} . On the other hand, if the interface runs along the direction perpendicular to the chain, the spin correlation along the chain decays exponentially like that in the case of the nearest-neighbor ferromagnetic Ising model. Thus the previous MHZ theory gives the

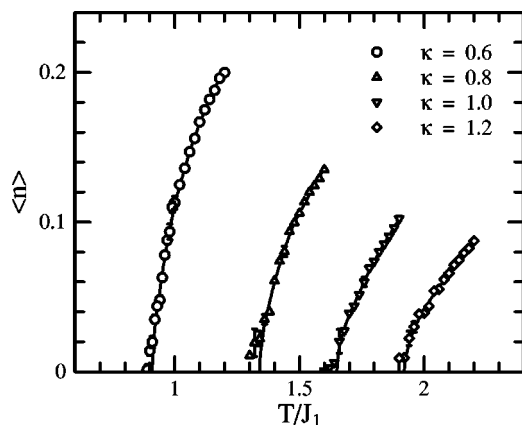


FIG. 16. The temperature dependences of the extrapolated density $\langle n \rangle$ of the domain walls for different κ . The lines are guides to the eyes.

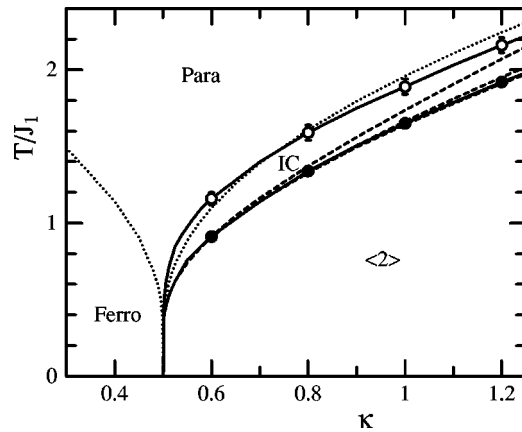


FIG. 17. The phase diagram of the ANNNI model with $J_0=J_1$. Open and filled circles indicate T_{c1} and T_{c2} , respectively, and lines are guides to the eyes. The dotted curve is the result of the MHZ theory of Ref. 15, and three broken curves are, from below, those of our MHZ theory, the fermion approximation of VB (Ref. 3) and that of GC (Ref. 13).

upper transition temperature T_{c1} . Of course, these arguments hold when these two types of the instability of the $\langle 2 \rangle$ phase occur separately. If one occurs at a lower temperature, then the other will follow in somewhat different manner. In fact, T_{c1} obtained by the present MC study is slightly different from that of the previous MHZ method.

V. CONCLUSIONS

The ANNNI model in two dimensions is a prototype of systems with competitive interactions. It has been believed that a floating IC phase appears between the $\langle 2 \rangle$ phase and the paramagnetic phase. However, both higher and lower transition temperatures T_{c1} and T_{c2} have not yet been established because of the difficulty of numerical calculations.

In this paper, we have developed an efficient method for obtaining equilibrium properties of the model. We find that the phase transition at T_{c1} is well described by the Kosterlitz-Thouless theory, and that at T_{c2} by the fermion approximations. Applying the finite-size scaling analyses, we determine T_{c1} and T_{c2} in a good accuracy. In contrast to the previous suggestions, T_{c2} is well described by the fermion approximations which concern with the instability of the $\langle 2 \rangle$ phase against the creation of the $+++$ or $---$ domain walls along the chain direction. On the other hand, T_{c1} is approximately described by the previous MHZ theory which concerns with the instability of the $\langle 2 \rangle$ phase against the formation of the interface along the axial direction.

Therefore we may roughly say on the unusual spin ordering of the ANNNI model with $\kappa > 1/2$: as the temperature is increased, those two instabilities occur successively at T_{c2} and T_{c1} . At intermediate temperatures ($T_{c2} < T < T_{c1}$), the $\langle 2 \rangle$ phase is unstable but a strong spin correlation still remains in the chains, because the interface along the axial direction are still absent. This is the origin of the appearance of the IC phase. As the temperature approaches to T_{c1} , a number of the domain walls along the chain are created and the spin structure is strongly deformed. Then dislocations of

•	•	•	•	•	•	•	
•	•	•	•	•	•	•	
6	-	-	-	-	-	-	
5	+	+	+	+	+	+	
4	+	+	+	+	+	+	
3	-	-	+	+	-	-	
2	-	-	-	-	-	-	
1	+	-	-	-	+	+	•••
0	+	+	+	+	+	+	
-1	+	+	+	+	+	-	
-2	-	-	-	-	-	-	
-3	-	-	-	-	-	-	
-4	+	+	+	+	+	+	
•	•	•	•	•	•	•	
•	•	•	•	•	•	•	
	n_1	n_2	n_3	n_4	n_5	n_6	

FIG. 18. An example of spin configurations considered in Eq. (18).

the network of the domain walls will also be possible. If this instability of the IC phase occurs at T_{c1} , the phase transition will exhibit the KT nature as discussed by Villain and Bak.³ These considerations explain our MC results. An interesting problem which remains unsolved is the location of the Lifshitz point at which T_{c1} and T_{c2} come together. One has believed that it exists at $\kappa = \kappa_c \leq 1.0$,^{3,8} but we could not find it up to $\kappa = 1.2$, as shown in Fig. 17. Moreover, our preliminary calculations have suggested its absence up to $\kappa = 2.0$. Then we think that κ_c will be much larger than that believed previously, if it even exists.

Finally, we should note that the results in this paper are obtained within a reasonable computer CPU time by using the CHB method. The method is particularly effective for analyzing properties of complex Ising systems such as Ising spin-glasses.^{20,21} The method is also applicable for analyzing different models with discrete spin variables such as the Potts and chiral clock models.

ACKNOWLEDGMENTS

The authors wish to give their thanks to Professor S. Fujiki for showing them unpublished data of the ANNNI model and for useful comments. They also wish to thank Professor T. Shirakura and O. Koseki for valuable discussions on the application of the CHB method, Dr. N. Suzuki for helping numerical calculations, and Professor K. Sasaki and Dr. T. Nakamura for a critical reading of the manuscript.

APPENDIX

Here we consider a lattice with open boundary conditions for both directions. Kroemer and Pesch calculated the interface free energy using the Müller-Hartmann and Zittartz (MHZ) method. They considered the interface along the axial direction (type Y). In that case, the loss of the interface energy is $2J_0$ for every chain. Another type of the interface exists, which runs along the chain direction (type X). In this case, two domain walls are created simultaneously and the resulting energy loss is $2(-J_1 - 2J_2) = 2J_1(2\kappa - 1)$ for every column in the axial direction, because the spin configuration in the axial direction changes from $++\cdots--$ to $++\cdots++$ due to the pinning effect.¹⁶ Of course, in a very large lattice, we can neglect interactions of those domain walls. Thus, at least for $J_1(2\kappa - 1) < J_0$, the interface of type X will be more likely to appear when the temperature is increased.

We can readily calculate the wall formation free energy when the interaction of domain walls can be neglected. Suppose that, for every column in the axial direction, two $\langle 2 \rangle$ spin configurations are separated by only one $+++$ or $---$ domain wall, as shown in Fig. 18. We denote the position of the center of the domain wall as n_i for the i th column. Suppose $n_1 = n_L = 0$, then $n_i = 0, \pm 2, \pm 4, \dots$, because the position of the domain wall changes by ± 2 when the spin on an edge of the domain wall is reversed. Then the energy of this domain wall with column positions $\{n_i\}$ with respect to the $\langle 2 \rangle$ phase is

$$E(\{n_i\}) = J_1(2\kappa - 1)L + J_0 \sum_{i=1}^{L-1} |n_{i+1} - n_i|. \quad (\text{A1})$$

The calculation of the free energy σ of this domain wall is straightforward,¹⁴ and the result is given as

$$\sigma/L \sim J_1(2\kappa - 1) - T \ln \left(\frac{1 + \exp(-2J_0/T)}{1 - \exp(-2J_0/T)} \right). \quad (\text{A2})$$

From $\sigma = 0$, we obtain the equation of the melting temperature of the $\langle 2 \rangle$ phase as

$$\sinh \left(\frac{J_1(2\kappa - 1)}{T_{c2}} \right) \sinh \left(\frac{2J_0}{T_{c2}} \right) = 1. \quad (\text{A3})$$

This equation reproduces that of Villain and Bak in the case $\kappa \rightarrow 0.5$.

¹For example see, e.g., W. Selke, in *Phase Transitions and Critical Phenomena*, edited by C. Domb and J. L. Lebowitz (Academic Press, New York, 1992), Vol. 15, p. 1, and references therein.

²W. Selke and M.E. Fisher, *Z. Phys. B* **40**, 71 (1980).

³J. Villain and P. Bak, *J. Phys. (Paris)* **42**, 657 (1981).

⁴M.A.S. Saqi, and D.S. McKenzie, *J. Phys. A* **20**, 471 (1987).

⁵Y. Murai, K. Tanaka, and T. Morita, *Physica A* **217**, 214 (1995).

⁶W. Selke, *Z. Phys. B* **43**, 335 (1981).

⁷W. Selke, K. Binder, and W. Kinzel, *Surf. Sci.* **125**, 74 (1983).

⁸J. Oitmaa, *J. Phys. A* **18**, 365 (1985).

⁹P.D. Beale, P.M. Duxbury, and J. Yeomans, *Phys. Rev. B* **31**, 7166 (1985).

¹⁰M.D. Grynberg and H. Ceva, *Phys. Rev. B* **36**, 7091 (1987).

¹¹M.N. Barber and B. Derrida, *J. Stat. Phys.* **51**, 877 (1988).

¹²J.M. Kosterlitz and D.J. Thouless, *J. Phys. C* **6**, 1181 (1973).

¹³M.D. Grynberg and H. Ceva, *Phys. Rev. B* **43**, 13 630 (1991).

¹⁴E. Müller-Hartmann and J. Zittartz, *Z. Phys. B* **27**, 261 (1977).

¹⁵J. Kroemer and W. Pesch, *J. Phys. A* **15**, L25 (1982).

¹⁶W. Selke and M.E. Fisher, *Phys. Rev. B* **20**, 257 (1979).

¹⁷O. Koseki and F. Matsubara, J. Phys. Soc. Jpn. **66**, 322 (1997).

¹⁸F. Matsubara, A. Sato, O. Koseki, and T. Shirakura, Phys. Rev. Lett. **78**, 3237 (1997).

¹⁹V.L. Pokrovsky and A.L. Talapov, Phys. Rev. Lett. **42**, 65 (1979).

²⁰T. Shirakura and F. Matsubara, Phys. Rev. Lett. **79**, 2887 (1997).

²¹F. Matsubara, T. Shirakura, and M. Shiomi, Phys. Rev. B **58**, R11 821 (1998).